Heliyon 10 (2024) e24202

Contents lists available at ScienceDirect

Heliyon

journal homepage: www.cell.com/heliyon

Research article

Synthesis and biological activity of imidazole phenazine derivatives as potential inhibitors for NS2B-NS3 dengue protease

Nur Sarah Dyana Khalili [a,b], Muhammad Hidhir Khawory [a,**], Nurul Hanim Salin [a], Iffah Izzati Zakaria [c], Maywan Hariono [d], Andrey A. Mikhaylov [e], Ezatul Ezleen Kamarulzaman [a,d], Habibah A Wahab [a,d], Unang Supratman [f], Mohamad Nurul Azmi [b,*]

[a] *Malaysian Institute of Pharmaceuticals and Nutraceuticals, National Institutes of Biotechnology Malaysia, Gelugor, Pulau Pinang, Malaysia*
[b] *Natural Products and Synthesis Organic Research Laboratory (NPSO), School of Chemical Sciences, Universiti Sains Malaysia, 11800 Minden, Penang, Malaysia*
[c] *Malaysia Genome and Vaccine Institute, National Institutes of Biotechnology Malaysia, 43000 Kajang, Selangor, Malaysia*
[d] *School of Pharmaceutical Sciences, Universiti Sains Malaysia, 11800 Minden, Pulau Pinang, Malaysia*
[e] *Shemyakin-Ovchinnikov Institute of Bioorganic Chemistry of the Russian Academy of Sciences, 16/10 Miklukho-Maklaya St., Moscow, 117997, Russia*
[f] *Department of Chemistry, Faculty of Mathematics and Natural Sciences, Universitas Padjadjaran, 45363 Jatinangor, Indonesia*

ARTICLE INFO

Keywords:
Imidazole phenazines
Anti-dengue
DENV2 NS2B-NS3 protease
Molecular docking

ABSTRACT

A series of new imidazole-phenazine derivatives were synthesized via a two-step process. The condensation of 2,3-diaminophenazine and benzaldehyde derivatives proceeds with intermediate formation of an aniline Schiff base, which undergoes subsequent cyclodehydrogenation *in situ*. The structures of the synthesized compounds were characterized by 1D and 2D NMR, FTIR and HRMS. A total of thirteen imidazole phenazine derivatives were synthesized and validated for their inhibitory activity as anti-dengue agents by an in vitro DENV2 NS2B-NS3 protease assay using a fluorogenic Boc-Gly-Arg-Arg-AMC substrate. Two para-substituted imidazole phenazines, **3e** and **3k**, were found to be promising lead molecules for novel NS2B-NS3 protease inhibitors with IC_{50} of 54.8 μM and 71.9 μM, respectively, compared to quercetin as a control (IC_{50} 104.8 μM). The *in silico* study was performed using AutoDock Vina to identify the binding energy and conformation of **3e** and **3k** with the active site of the DENV2 NS2B-NS3 protease Wichapong model. The results indicate better binding properties of **3e** and **3k** with calculated binding energies of −8.5 and −8.4 kcal mol^{-1}, respectively, compared to the binding energy of quercetin of −7.2 kcal mol^{-1}, which corroborates well with the experimental observations.

1. Introduction

Dengue infections caused by the pathogenic *flaviviruses* transmitted by *Aedes aegypiti* and *Aedes albopictus*, to humans is a serious health concern globally [1]. In Malaysia alone, a cumulative 56,721 cases including 39 fatalities due to dengue was reported by the

* Corresponding author.
** Corresponding author.
E-mail addresses: muhammad_hidhir@nibm.my (M.H. Khawory), mnazmi@usm.my (M. Nurul Azmi).

https://doi.org/10.1016/j.heliyon.2024.e24202
Received 3 October 2023; Received in revised form 4 January 2024; Accepted 4 January 2024
Available online 8 January 2024

World Health Organization (WHO) by August 2023, an increase of 144.7 % compared to 23,183 cases and 16 deaths in the same period in 2022 [2]. Meanwhile, as of July 27, 2023, more than three million cases and over 1500 deaths related to dengue have been recorded worldwide, surpassing the 2.8 million dengue cases reported during the whole of 2022 [3].

The single-stranded positive-sense RNA genome of a *flavivirus* is translated into a polyprotein, which is subsequently cleaved by the host and the virus into three structural proteins (capsid, C; membrane, prM/M; and envelope, E) and seven non-structural proteins (NS1, NS2A, NS2B, NS3, NS4A, NS4B and NS5) [4]. In addition, the four major dengue virus serotypes DENV1, DENV2, DENV3 and DENV4 are the most important re-emerging arboviruses in terms of geographical distribution and frequency of infection [5]. Therefore, these distinct serotypes were thought to be the trigger of dengue fever, including dengue hemorrhagic fever, which in severe cases is usually fatal. In the absence of an appropriate treatment, severe dengue infection has a high morbidity and mortality rate [6].

The active site of the NS3 serine protease carries the catalytic triad comprising of three amino acid residues, namely HIS51, ASP75 and SER135. However, for optimal catalytic activity, NS2B must act as a cofactor of NS3 serine protease [7], as it contributes to the activity of NS3 through its hydrophobic region, where it participates in membrane attachment during the cleavage process, while the hydrophilic region retains and promotes the activation of NS3 [8]. The synthesis of the polyprotein precursor depends on the serine protease of the non-structural protein NS2B-NS3, which is critical for viral replication. Thus, this unique two-component NS2B-NS3 is an important target for the development of most anti-dengue drugs [9].

The design and development of several promising heterocyclic scaffolds as antiviral drug candidates for dengue virus (DENV) suppression has been driven by recent developments in medicinal chemistry. Previous studies have described quinoline [10], piperidone [11], thioguanine [12] and benzimidazole [13] as DENV2 NS2B-NS3 protease inhibitors. These compounds have an *N*-heterocyclic structure that could provide a good scaffold for such inhibitor. In this project, we are focusing on the hybrid compounds of phenazine and imidazole.

Phenazine is also a member of the *N*-heterocyclic compound. Most naturally occurring phenazines are derived from terrestrial and marine microbes [14]. These heteroaromatic, conjugated, nitrogen-containing systems are the building blocks of a variety of organic materials, both natural and synthetic [15]. In recent years, phenazines has widely attracted considerable attention due to their interesting biological activities such as antimalaria, antiprotozoal [16], antifungal [17] and antibiotic agents [18]. In addition, the development of phenazine derivatives as inhibitors of disease-related targets and their apparent activity in inhibiting enzymes such as tyrosine kinase [19] and topoisomerase [20] made them ideal for the purpose of this study. Despite the relevance of phenazine derivatives, there is still a dearth of information on their potential as inhibitors of DENV2 NS2B-NS3 protease. The only comparative research was observed *in silico*, where two nitro-benzylidene phenazine derivatives (Fig. 1A and **B**) with pharmacophore hit of 52 %–55 %, demonstrated their stability in the primary binding pocket of NS2B-NS3 protease with MM-PBSA binding energies ranging from −22.53 to −17.01 kcal mol^{-1}, indicating probable binding in DENV2 NS2B-NS3 protease [21].

Another aromatic heterocyclic scaffold is imidazole, which belongs to the class of five-membered cycle. An imidazole structure consists of three carbon atoms and two nitrogen atoms that are not vicinal to one another. Imidazole is amphoteric and highly polar by nature [22]. Due to their bioactivity, substituted imidazole scaffolds exhibit a wide range of biological activities, including antiviral, anti-HIV, analgesic, anticancer, anti-inflammatory, and antibiotic activities [23]. In 2018, Sucipto et al. proposed an imidazole

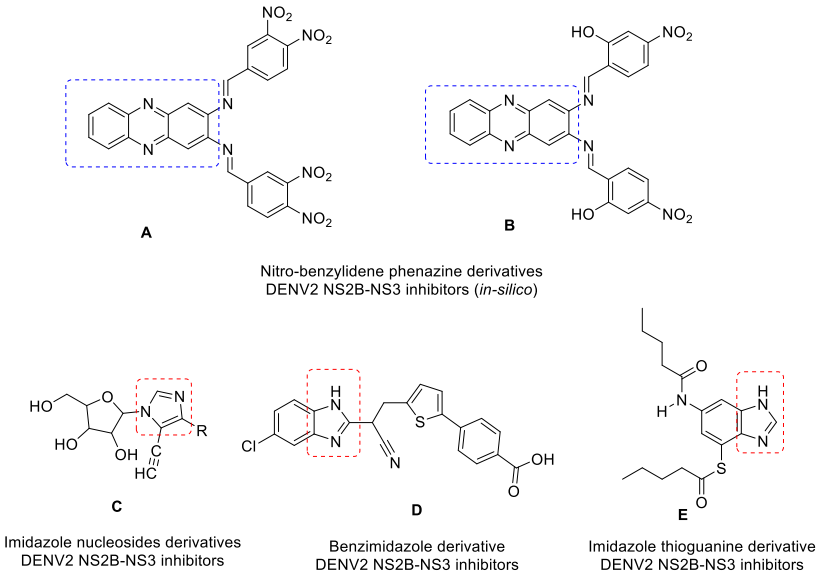

Fig. 1. Reported phenazine and imidazole motifs as anti-dengue inhibitors. (A) and (B) The nitro-benzylidene phenazine derivatives reported as potential inhibitors of DENV2 NS2B-NS3 (*in silico* study) [21]. (C) Imidazole nucleoside derivatives reported as DENV2 NS2B-NS3 inhibitor [25]. (D) The benzimidazole derivative studied as DENV2 NS2B-NS3 inhibitor [26]. (E) The investigated imidazole thioguanine derivative on DENV2 NS2B-NS3 inhibitory activities [12].

complex for anti-dengue inhibition for the first time [24]. A few more studies on imidazole scaffolds (Fig. 1C, **D** and **1E**) as dengue inhibitors was reported since then [12,25–27].

Imidazole phenazine derivatives was previously discovered as anticancer [28], antiproliferative [29], tuberculostatic [30] and chemsensor [31]. Amer et al. were the first to report this ligand in 1999 [32], which was later characterized spectroscopically by Lei and co-workers in 2011 with substituents varied on the terminal benzene ring [33]. In this article, we report the synthesis of imidazole phenazine derivatives, biological evaluation and *in silico* study on DENV2 NS2B-NS3 protease. This is the first updated study for this hybrid compound.

2. Results and discussions

2.1. Chemistry

The synthesis of imidazole phenazine with various substituents on the terminal benzene ring is shown in Scheme 1. This reaction initially proceeds by condensation 2,3-diaminophenazine with aldehyde in ethanol under reflux which then undergo an oxidative cyclization step to form the desired products **3a-3m**. The reaction conditions used herein reflux of 1 equiv. of diamine **1** with 2 equiv. of aldehyde **2** in ethanol. The result was supported by the manuscript published by Lin et al. [34]. In the current report, the process is catalyst-free and utilizes ethanol as a solvent, which is in accordance with the principles of green chemistry [35]. The reactions afforded the final compounds imidazoles **3a-3m** with various donating and acceptor substituents in the aromatic ring with a yield between 15 % and 90 %. However, the research is subject to a limitation, as all synthesized compounds have a melting point more than 300 °C. The melting points were measured using the Stuart SMP10 digital melting point instrument (Stuart Scientific Bibby Sterilin Ltd., UK), which can only measure temperature up to 300 °C. Thus, the exact range of melting points is unspecified in this manuscript.

A suggested mechanism for the synthesis of the imidazole phenazine derivatives **3a-3m** is depicted on Scheme 2. The nitrogen of the amine acts as a nucleophile and attacks the electrophilic carbonyl carbon of the benzaldehyde to form a Schiff base (C═N) and a water molecule displaced [36]. It then undergoes through a cyclization process in which the intramolecular nucleophilic attack on the imine carbon form 5-membered imidazoline ring. The latter is prone to fast oxidation into aromatic imidazole motif by action of air oxygen, which is well-documented in the literature [37–40].

The structural elucidation of imidazole phenazine hybrid **3a-3m** was carried out based on their spectrum including 1D and 2D

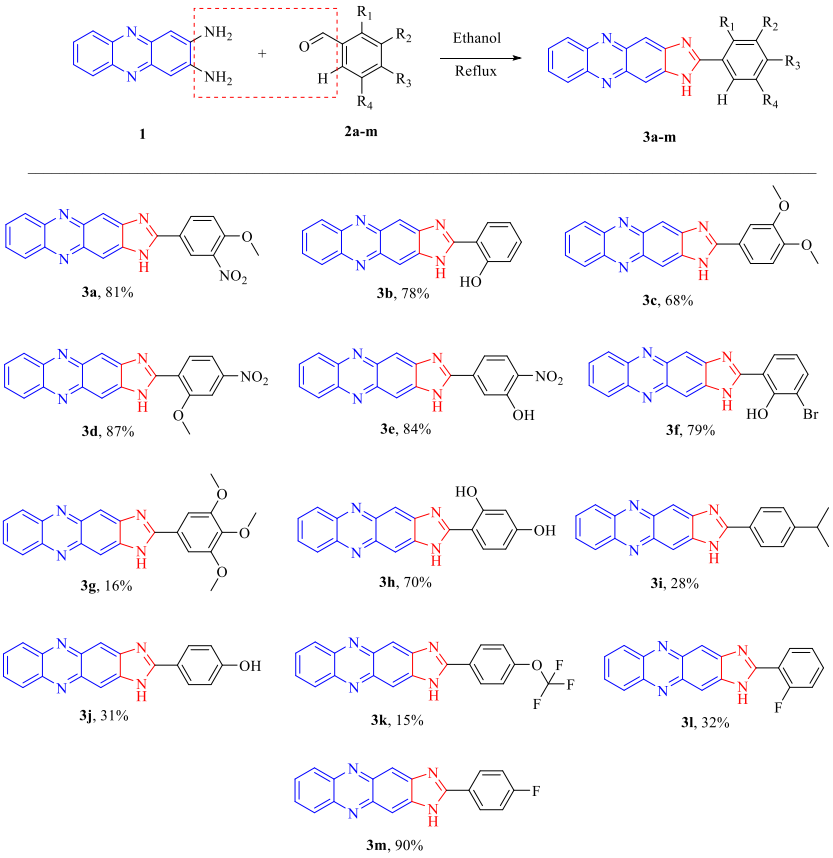

Scheme 1. Synthesis of imidazole phenazine derivatives **3a-3m**.

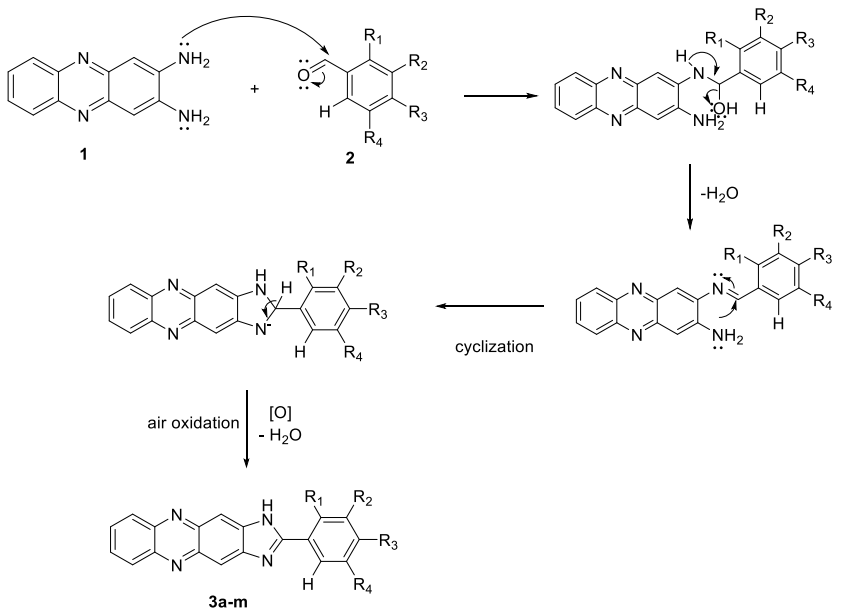

Scheme 2. Proposed mechanism for the formation of imidazole phenazine derivatives **3a-3m** via condensation reaction [41].

NMR, FTIR, and HRMS, and comparison with literature data for related compounds. The compound 2-(2,4-dihydroxyphenyl)-1H-imidazo [4,5-b]phenazine (**3h**), having a degree of unsaturation value of 16 was obtained as brownish orange solid and is used as a characteristic representative for further discussion of spectral data. The HRMS spectrum of compound **3h** exhibits molecular ion $[M+H]^+$ with *m/z* 329.1035, corresponding to the molecular formula $C_{19}H_{12}N_4O$ of imidazole compound with *m/z* 329.1039, confirmed the structural elucidation of **3h**. The IR absorptions at 3400, 3234, 3064, and 1631 that were correlated to the to N–H stretching, O–H stretching, C═C aromatic stretching, C–C bending, and C═N imidazole stretching, respectively.

The ^{1}H NMR data for the compound **3h** exhibits characteristic region of δ_H 6.49–13.26. The absence of the –NH_2 peak and the appearance of a singlet with integral of 1H in the δ_H 13.26 ppm correspond to the –NH group of the imidazole ring, which supports the structure of the product. Moreover, there is no singlet observed at δ_H 8.00, expected for the structure of the Schiff's base. The singlet peaks at δ_H 13.00 and 10.41 correspond to –OH group at *ortho* and *para* position of substituents benzene ring. The protons of the benzene ring were observed in the aromatic proton zone between δ_H 6.49–8.40. The structure was confirmed with ^{13}C NMR spectrum, which has a total number of 19 carbon signals exhibited in the aromatic zone at the range of δ_C 103.6–163.3.

Further structure elucidation for the compound **3h** is illustrated (Fig. 2): using 2D-NMR spectroscopy such as COSY, and HMBC the connectivity of the derivative hybrid between phenazine and imidazole moiety was established. The substitute terminal benzene on the core imidazole phenazine showed the aromatic proton of H-2′, H-5′, and H-6′ exhibited at δ_H 6.49 (d, J = 2.3 Hz), 8.04 (d, J = 8.6 Hz) and 6.55 (dd, J = 2.3, 8.6 Hz) respectively. The resonance of C-2′, C-5′, and C-6′ in HSQC was assigned at δ_C 103.6, 129.9, and 109.0, respectively. The neighbouring proton correlation was revealed by the ^{1}H–^{1}H–COSY spectrum. The protons of phenazine ring displayed cross-peaks between protons assign at δ_H 7.89–7.88 (H-13, H-14) to their neighbouring protons at δ_H 8.24–8.23 (H-12, H-15). Another proton-proton correlation, H-5′ with H-6′ are observed within the substitute benzene ring system. HMBC spectrum which signified correlations between the protons to carbons showed that the skeletal framework of phenazine is confirmed by the cross-correlation of H-6, H-9, H-13 and H-14 with δ_C 140.8 (C-7), δ_C 140.7 (C-8), δ_C 142.1 (C-11), and δ_C 142.2 (C-10), respectively. In addition, H-6 showed the correlation with δ_C 139.4 (C-5) and H-9 with δ_C 147.2 (C-4) confirm the connectivity of phenazine group and imidazole ring. The cross-correlation of H-5′ with δ_C 160.7 (C-2) revealed the linked terminal benzene ring substituent attached to the 2-imidazole group. The presence of *ortho* and *para* substituted benzene-diol group was further proof by correlation of H-2′ with C–OH δ_C 161.9 (C-3′), H-6′ with δ_C 104.2 (C-4′) and O–H′ at δ_H 10.41 was seen to correlated with δ_C 103.6 (C-2′) and δ_C 129.3 (C-6′).

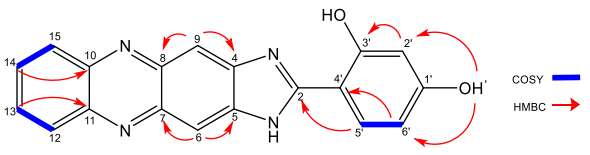

Fig. 2. COSY and HMBC correlations of compound **3h**.

2.2. Biology

2.2.1. DENV2 NS2B-NS3 protease inhibitory assay

The protease and substrate concentrations used in this assay were 3.5 μM and 150 μM, respectively (see Supporting Information S40 for more details). First, screening of all synthesized compounds **3a-3m** at 700 μM was performed using the optimized dengue protease assay to estimate the inhibitory activity of the sample compounds. It was found that all compounds inhibited dengue protease at 700 μM by more than 50 % except **3b** (Table 1 and Fig. 3).

The half-maximal inhibitory concentration (IC_{50}) values of the compounds with more than 50 % inhibition at 700 μM were determined at different concentrations in a range of 5.5–700.0 μM. Quercetin was selected as a positive control mainly because of its established antiviral capabilities and prior correlation with dengue virus suppression as it has been previously reported against DENV2 and impaired virus replication in cells [42]. Thus, using quercetin as a control in an NS2B-NS3 dengue protease inhibition assay to evaluate a synthesized compound may be a valid approach. It can help validate the assay, performance by providing a reference point for inhibition.

Compounds **3e** and 3**k**, having a nitro group (–NO_2) and a trifluoromethoxy group (–OCF_3) at the para-position of the benzene substituent, displayed some level of inhibition of DENV2 NS2B-NS3 protease showed most potency in comparison to other derivatives with IC_{50} values of 54.8 μM and 71.9 μM, respectively, compared to quercetin ($IC_{50} = 104.8$ μM) (Fig. 4). This suggests that both **3e** and **3k** have the potential to be developed as anti-dengue drugs. Meanwhile, compounds **3a**, **3d**, **3f** and **3i** show slightly strong inhibition against DENV2 NS2B-NS3 with IC_{50} of 85.9 μM, 79.0 μM, 92.7 μM and 92.1 μM, respectively. Nonetheless, other derivatives show moderate inhibition with $IC_{50} > 100$ μM (Table 2).

2.3. Molecular docking

The two potent imidazole phenazine were then investigated for their ΔG_{bind} and further understanding on the binding mechanism of the anti-dengue effect via a molecular docking approach. The interaction and binding energy were performed between the compounds and the active site of DENV2 NS2B-NS3 protease Wichapong model [43]. This model has been successfully used in the search for hits used in some projects for the discovery of DENV2 NS2B-NS3 protease inhibitors with thioguanine [7,12], malabaricon, acylphenol [44] and benzofuranone [45]. The use of a homology model, a reliable 3D model generated from its amino acid sequence, is acceptable for computational analysis [46]. Table 3 summarizes the binding energies of the docked DENV2 NS2B-NS3 protease with **3e** and **3k**, while Table 4 shows the specific types of binding interactions. The calculated lowest binding energy between **3e** and DENV2 NS2B-NS3pro is -8.50 kcal mol^{-1}, while **3k** is -8.4 kcal mol^{-1}.

The synthesized imidazole phenazine **3e** showed six hydrogen bonds and five hydrophobic interactions with the active site of DENV2 NS2B-NS3 protease. **3e** showed three conventional hydrogen bonds interactions, where one of it exhibited between the hydrogen atom of –NH on the imidazole ring with B:GLY151, while two other hydrogen bonds interacted with the hydrogen atom of the hydroxyl group on the substituted phenyl ring with A:GLY82 and B:ASN152. Meanwhile, a carbon-hydrogen bond is formed between B:TRP50 and the oxygen atom of the nitro group. Furthermore, the interaction between phenyl group of the phenazine and imidazole ring with B:TRY161 and B:HIS51, respectively, was recognized as a π-donor hydrogen bond. The hydrophobic interaction was linked by the binding of substituent phenyl, and imidazole ring via π-π stacked and π-π T-shaped interactions respectively with B:HIS51. In addition, π-π stacked interaction also occurred between phenazine as a whole with B:TRY161. The binding was also stabilized through van der Waals forces of **3e** with A:ASP81, B:TRP50, B:VAL72, B:ASP75, A:SER83, B:SER135, B:PHE130, B:ASP129, and B:VAL155 (Table 4, Fig. 5A).

Another potential anti-dengue compound, **3k**, displayed three hydrogen bonds interaction where, one carbon hydrogen bond observed between the fluorine atom of the trifluoromethoxy and the B:TRP50. The interaction of the π-donor H-bond was observed between the pyrazine of phenazine and B:TYR161. Another π-donor H-bond was found between the imidazole ring and B:HIS51. A halogen bond was also formed between the fluorine atom of the trifluoromethoxy group with three amino acid residues, A:ASP81, B:VAL72 and B:ASP75. Meanwhile, the carbon atom of the trifluoromethoxy group formed an alkyl and π-alkyl interaction with B:VAL72 and B:TRP50, respectively. The main block, imidazole phenazine, formed a similar hydrophobic interaction as **3e**. Phenazine and B:TRY161 were linked via a π-π stacking interaction. The substituent phenyl and the imidazole ring bind with B:HIS51 via π-π stacked and π-π T-shaped interactions, respectively. The van der Waals forces stabilized the binding of **3k** with A:GLY82, B:ASN152, B:GLY151, B:SER135, B:PHE130, and B:ASP129 (Table 4, Fig. 5B).

Table 1
Percentage of enzyme activity and inhibition of imidazole phenazine derivatives at 700 μM in DMSO.

Compd.	% inhibition	Compd.	% inhibition
3a	83.50 ± 1.96	**3h**	84.70 ± 1.26
3b	46.65 ± 1.68	**3i**	75.68 ± 0.26
3c	55.31 ± 0.39	**3j**	60.27 ± 2.27
3d	83.88 ± 1.67	**3k**	63.32 ± 2.80
3e	95.46 ± 1.75	**3l**	78.23 ± 0.03
3f	70.85 ± 1.46	**3m**	84.75 ± 0.89
3g	53.28 ± 2.76	**Quercetin (Control)**	90.27 ± 0.49

± standard deviation for n = 3 experiments.

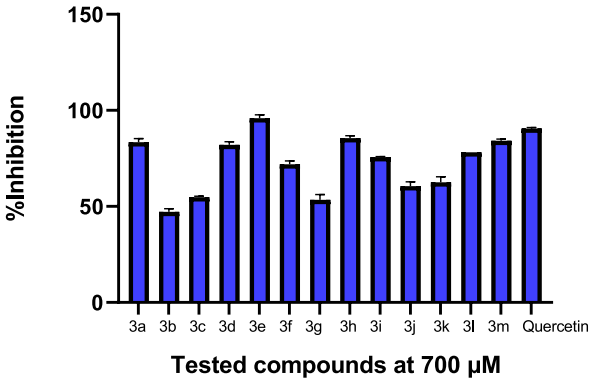

Fig. 3. Histogram representing the percentage of inhibition of the synthesized imidazole phenazine derivatives compared to the positive control (quercetin) at 700 µM.

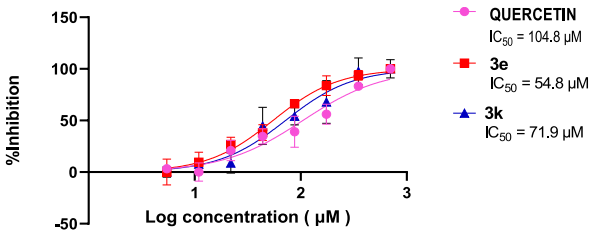

Fig. 4. Dose response curves of compounds **3e** and **3k** compared to the positive control (Quercetin) on NS2B/NS3 proteases.

Table 2
The list of imidazole phenazine derivatives with their experimental **IC_{50}** against DENV2 NS2B-NS3pro.

Compd.	R_1	R_2	R_3	R_4	IC_{50} (µM)
3a	H	NO_2	OCH_3	H	85.9 ± 6.9
3b	OH	H	H	H	ND
3c	H	OCH_3	OCH_3	H	129.3 ± 6.7
3d	OCH_3	H	NO_2	H	79.0 ± 7.9
3e	H	OH	NO_2	H	54.8 ± 7.1
3f	OH	Br	H	H	92.7 ± 6.2
3g	H	OCH_3	OCH_3	OCH_3	136.3 ± 8.0
3h	OH	H	OH	H	147.1 ± 22.9
3i	H	H	$CH(CH_3)_2$	H	92.1 ± 6.9
3j	H	H	OH	H	183.9 ± 15.2
3k	H	H	OCF3	H	71.9 ± 8.0
3l	F	H	H	H	168.8 ± 0.5
3 m	H	H	F	H	158.2 ± 16.3
Quercetin					104.8 ± 25.6

± standard deviation for n = 3 experiments.
Abbreviation: ND, not determined.

Table 3
In vitro inhibition and *in silico* binding energy of the potent synthesized compounds on DENV2 NS2B-NS3 protease.

Compd.	IC_{50} (µM)	ΔG_{bind} (kcal mol^{-1})
3e	54.77	−8.50
3k	71.88	−8.40
Quercetin	104.80	−7.20

It was discovered that the NS3 residues with different interaction type and strength contributed most to the interactions between the inhibitors and the active site of DENV2 NS2B-NS3 Wichapong model, including HIS51, ASP75 and SER135, which are the standard catalytic triad of NS3 protein residues. Virion development and viral replication depend on NS3 protein residues. Nevertheless, the

Table 4
The key interactions of the compounds **3e** and **3k** with the amino acids of NS2B-NS3pro Wichapong model.

Enzyme	Cpd.	Protein residue	Interaction unit of the compound	Distance (Å)	Type of interactions	vdW Interactions
NS2B-NS3pro (Wichapong model)	**3e**	B:GLY151	Imidazole	3.01	H Bond	A:ASP81, B:TRP50, B:VAL72, B:ASP75, A:SER83, B:SER135, B:PHE130, B:ASP129, B:VAL155
		A:GLY82	Phenyl	2.22	H Bond	
		B:ASN152		2.79	H Bond	
		B:TRP50	NO_2	2.77	Carbon H Bond	
		B:TYR161	Phenyl of phenazine	3.24	π-Donor H Bond	
		B:HIS51	Imidazole	2.54	π-Donor H Bond	
		B:HIS51	Phenyl	4.19	π-π Stacked	
		B:TYR161	Phenyl of phenazine	3.70	π-π Stacked	
		B:TYR161	Pyrazine of phenazine	4.18	π-π Stacked	
		B:TYR161	Phenyl of phenazine	5.61	π-π Stacked	
		B:HIS51	Imidazole	4.52	π-π T-shaped	
	3k	B:TRP50	OCF_3	2.26	Carbon H Bond	A:GLY82, B:ASN152,
		A:ASP81		3.57	Halogen	B:GLY151,
		B:VAL72		3.50	Halogen	B:SER135,
		B:ASP75		3.42	Halogen	B:PHE130,
		B:TYR161	Pyrazine of phenazine	2.99	π-Donor H Bond	B:ASP129
		B:HIS51	Imidazole	2.34	π-Donor H Bond	
		B:HIS51	Phenyl	4.65	π-π Stacked	
		B:TYR161	Phenyl of phenazine	3.69	π-π Stacked	
		B:TYR161	Pyrazine of phenazine	4.39	π-π Stacked	
		B:HIS51	Imidazole	4.44	π-π T shaped	
		B:VAL72	OCF_3	4.72	Alkyl	
		B:TRP50		4.75	π-Alkyl	
	Quercetin	B:SER135	OH pyranone	2.58	H bond	B:PHE130, B:ASP129, B:VAL155, B:GLY153, B:ASN152, B:ASP75
		B:GLY151	OH pyranone	2.76	H bond	
		B:TYR150	OH phenol	3.08	H bond	
		B:HIS51	Phenyl	4.28	π-π Stacked	
		B:TYR161	Pyranone	4.14	π-π Stacked	
			Phenol	3.79	π-π Stacked	

region of NS2B is also required for catalytic activity [47]. Therefore, it is suggested that having more interaction with the residue will lead to a better result in the inhibitory activity. Furthermore, to create the stable energy-favored ligands at the interface of a protein structure and alter the binding affinity for the drug efficacy, it was crucial to observe the hydrogen bonding and optimize the hydrophobic interactions [48]. It was found that both **3e** and **3k** showed more hydrogen bonding interactions with NS2B-NS3pro compared to quercetin (Table 4). These findings indicate that the results of the *in vitro* study are consistent with the *in silico* studies.

2.4. Structure-activity relationship studies (SARs)

The structure-activity relationship studies were performed to identify the effect between the chemical structure of the synthesized compounds and their potential against the DENV2 NS2B-NS3 protease based on the IC_{50} values (see Table 2). As explained in Section 2.3, it is suggested that the primary building block, imidazole phenazine, forms a hydrophobic interaction with the NS2B-NS3pro, as the phenazine and B:TRY161 are linked via a π-π stacking interaction. In contrast, the terminal phenyl ring and the imidazole ring bind to one of the catalytic triads B:HIS51 via π-π-stacking and π-π-T-shaped interactions, respectively. The different substituents on the terminal benzene ring alter the inhibition potency of the synthesized compound.

Para-substituted compounds have been found to have advantages in molecular interactions with the NS2B-NS3 protease. These advantages include lower steric hindrance, favorable electrostatic interactions, optimal conformation, π-π stacking, and hydrophobic complementarity. Compound **3e** with a substituted nitro group (–NO_2) on the para-position and hydroxy group (–OH) on the meta-position of the benzene ring exhibits the most promising DENV2 NS2B-NS3 inhibitory activity (IC_{50} = 54.8 μM). However, when the hydroxy group was removed and replaced by a methoxy group (−OCH_3) in ortho-position **3d**, the inhibitory activity is reduced by 1.4-fold (IC_{50} = 79.0 μM). When the nitro group was shifted from the para to the meta position and the para-position was replaced by –OCH_3 **3a**, the inhibitory activity also decreased slightly by 1-fold (IC_{50} = 85.9 μM).

Subsequently, the imidazole phenazine with substituted trifluoromethoxy (–OCF_3) on the para-position phenyl ring **3k** also showed a great inhibition activity (IC_{50} = 71.9 μM μM). Replacement with *tert*-butyl (–$CH(CH_3)_2$) **3i** reduces the activity by a fold (IC_{50} = 92.1

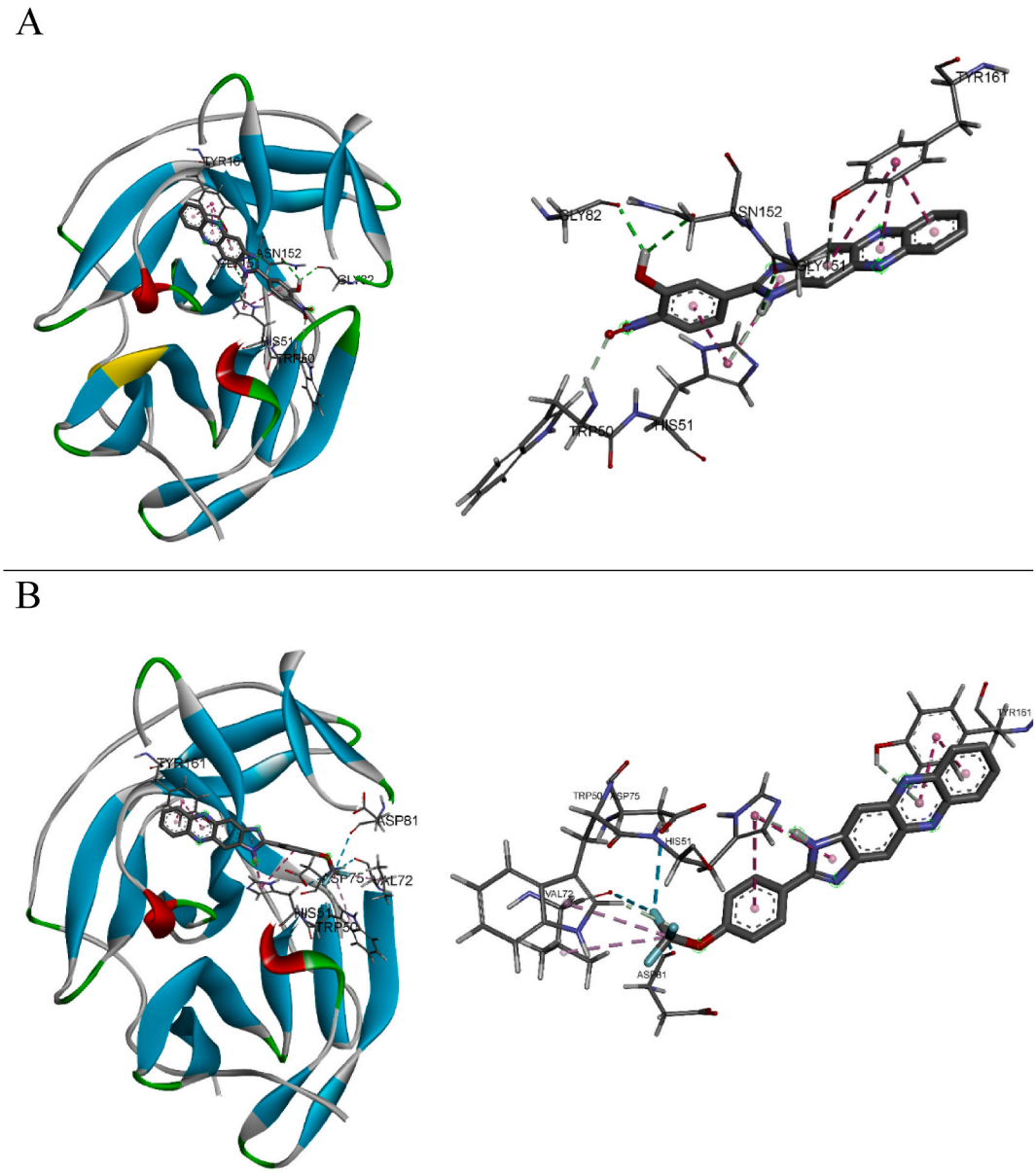

Fig. 5. The three-dimensional binding modes of compounds **3e** (A) and **3k** (B) are presented at the active site of NS2B-NS3 protease.

μM). In contrast, when the substituent at the para-position of the benzene ring is replaced by fluorine (−F) **3m**, the inhibition is decreases by 2.2-fold (IC_{50} = 158.2 μM) and moving the fluorine to the ortho-position **3l**, further reduced the inhibition activity (IC_{50} = 168.8 μM). The compound with the hydroxyl group at the para-position of the phenyl ring **3j** exhibits lowest inhibitory activity (IC_{50} = 183.9 μM) compared to the other imidazole phenazine derivatives, with a decrease 3-fold contrast to **3e**.

Consistent with the molecular docking study of **3e** and **3k**, the carbon-hydrogen interactions between the para-position NO_2 and OCF_3 of compounds **3e** and **3k**, respectively, are formed with the NS3 residue of TRP50. The electron-withdrawing nature of the NO_2 and OCF_3 groups enables them to form polar interactions with the protease through hydrogen bonding. Furthermore, the additional presence of meta-position hydroxyl group on the substituted phenyl ring of **3e** forms hydrogen bonds with A:GLY82 and B:ASN152, explains the better inhibition of **3e** compared to **3k**.

In short, we notice significance of the presence of an electron-withdrawing group and the positioning of the substituent, especially on the phenyl ring in para-position, exerts a positive influence on binding and inhibitory activity in the DENV2 NS2B-NS3 protease. NO_2 and OCF_3 are stronger electron-withdrawing groups due to the presence of highly electronegative elements such as nitrogen and fluorine. Although $CH(CH_3)_2$ withdraws electrons, it is weaker compared to NO_2 and OCF_3. OH, is an electron-donating group, and both F and OCH_3 are relatively weak electron-withdrawing groups compared to the other groups in the list. Nevertheless, the substituent at ortho- and meta-position on the benzene ring also influences the effectiveness of the inhibitory activities. Fig. 6 summarizes

the structure-activity relationships (SARs) studies of these imidazole phenazine derivatives.

3. Conclusion

A series of imidazole phenazine hybrids were synthesized, with yields ranging from 15 % to 90 %. Thirteen compounds were tested for their inhibition of DENV2 NS2B-NS3 protease, and two compounds, **3e** and **3k**, showed significant inhibitory activity with IC_{50} values of 54.8 μM and 71.9 μM, respectively. Molecular docking confirmed their binding to the target site. The study concludes that compounds **3e** and **3k** could be potential anti-dengue candidates, affirming further *in vivo* studies and lead structure optimization. Additionally, the study presents a convenient and environmentally benign method for the synthesis of imidazole phenazine by the reaction of substituted 2,3-diaminophenazine with benzaldehyde in a straightforward one-pot reflux process which might be beneficial for future studies and upscaling.

4. Materials and methods

4.1. Chemistry

All materials and chemicals, 2,3-diaminophenazine, 4-methoxy-3-nitrobenzaldehyde, 2-hydroxybenzaldehyde, 3,4-dimethoxybenzaldehyde, 2-methoxy-4-nitrobenzaldehyde, 3-hydroxy-4-nitrobenzaldehyde, 3-bromo-2-hydroxybenzaldehyde, 3,4,5-trimethoxybenzaldehyde, 2,4-dihydroxybenzaldehyde, 4-isopropylbenzaldehyde, 4-hydroxybenzaldehyde, 4-trimethoxybenzaldehyde, 2-fluorobenzaldehyde, 4-fluorobenzaldehyde, and ethanol were purchased from Sigma-Aldrich Co., Merck Chemical Co., and Fine Chemical Co. All chemicals were used without further purification unless stated otherwise. The reactions were carried out in dried glassware under the exclusion of moisture. Thin-layer chromatography investigation was performed on silica gel 60 F_{254}. Visualization was done by Ultraviolet light (254 nm). The nuclear magnetic resonance experiments were conducted using 700 MHz ASCEND spectrometer and Advance Bruker 500 MHz (Bruker Bioscience, Billerica, MA, USA). The data were analyzed using Top Spin 3.6.2 software package and chemical shifts were established in ppm referring to the solvent signals in DMSO-d_6 (^{1}H δ 2.50; ^{13}C δ 39.50). The infrared (IR) spectra were recorded through PerkinElmer FT-IR spectrometer RX1 (ATR) and Shimadzu FTIR spectrometer (KBr pellets). The mass spectra is reported in *m/z* were obtained by a Waters Xevo QTOF MS. Melting points were measured via the Stuart SMP10 digital melting point apparatus (Stuart Scientific Bibby Sterilin Ltd., UK).

4.1.1. Synthesis of imidazole phenazine derivatives

The synthesis of imidazole derivatives began with a condensation reaction between 2,3-diaminophenazine (**1**) and benzaldehyde derivatives **2.** As illustrated in Scheme 1, an absolute ethanol solution (10 mL) of 2,3-diaminophenazine (1 equiv.) was added to an absolute ethanol solution (10 mL) of substitute benzaldehyde (2 equiv.) in a 50 mL round bottom flask equipped with a condenser, a drying tube, a thermometer and a magnetic stirrer. The mixture was refluxed at 78 °C for 24–48 h at constant stirring and monitored using TLC. The precipitates formed were collected by filtration and washed with absolute ethanol. The resulting solid was dried in vacuo to obtain the pure compound in the yield of 15 %–90 %. The purity was determined using TLC with the solvent system of hexane to ethyl acetate in a ratio of 3:7. All synthesized compounds were characterized by various spectroscopic methods such as NMR, FTIR and HRMS. (see supplementary information for more details).

2-(4-methoxy-3-nitrophenyl)-1H-imidazo [*4,5-b*]*phenazine (**3a**)*: Yellowish orange solid (81 % yield); M.p. >300 °C; **FTIR** (cm^{-1}) 3361 (N–H), 3059 (Aromatic C–H), 2992 (C^3_{sp}–H), 1657 (C═N), 1624 (C═C), 1519 (–NO_2), 1422 (C–N), 1266 (C–O); **^{1}H NMR** (700 MHz, DMSO-d_6) δ 13.53 (s, N–H, 1H), 8.87 (d, J = 2.2 Hz, 1H), 8.62 (dd, J = 2.2, 8.8 Hz, 1H), 8.49 (s, 1H), 8.26 (s, 1H), 8.21–8.20 (m, 2H), 7.89–7.88 (m, 2H), 7.68 (d, J = 8.8 Hz, 1H), 4.07 (s, 3H); **^{13}C NMR** (175 MHz, DMSO-d_6) δ 158.3, 158.1, 155.1, 149.2, 142.4, 142.3, 140.9, 140.8, 139.7, 134.2, 130.4, 130.2, 129.5, 129.3, 125.0, 121.6, 115.9, 115.3, 106.6, 57.8; **HRMS** (+ESI) $[M+H]^+$: 372.1090, $C_{20}H_{13}N_5O_3$ requires 372.1096.

2-(2-hydroxyphenyl)-1H-imidazo [*4,5-b*]*phenazine (**3b**)*: Yellow solid (78 % yield); M.p. >300 °C. **FTIR** (cm^{-1}): 3305 (N–H/O–H), 3050 (Aromatic C–H), 1625 (C═N), 1531 (C═C), 1430 (C–N); **^{1}H NMR** (500 MHz, DMSO-d_6) δ 13.55 (s, N–H, 1H) 12.92 (s, O–H, 1H), 8.56 (s, 1H), 8.35 (s, 1H), 8.27–8.25 (m, 3H), 7.23–7.91 (m, 2H), 7.57–7.53 (m, 1H), 7.16 (d, J = 8.4 Hz, 1H), 7.14 (t, J = 7.2 Hz, 1H); **^{13}C NMR** (125 MHz, DMSO-d_6) δ 160.1, 159.7, 142.4, 142.3, 140.7, 140.6, 139.5, 139.2, 134.4, 130.5, 130.4, 129.5, 129.4, 128.5,

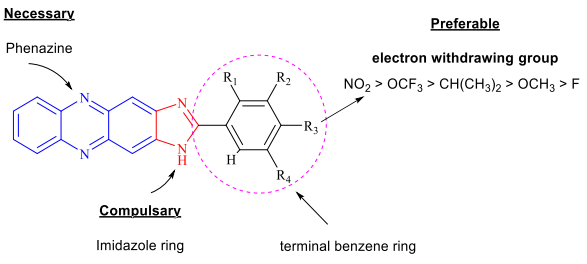

Fig. 6. Structure-activity relationships (SARs) studies of imidazole phenazine.

120.1, 118.0, 114.5, 112.4, 106.9; **HRMS** (+ESI) $[M+H]^+$: 313.1086, $C_{19}H_{12}N_4O$ requires 313.1089.

2-(3,4-dimethoxyphenyl)-1H-imidazo [*4,5-b*]*phenazine* ***(3c)***: Brownish yellow solid (68 % yield); M.p. >300 °C; **FTIR** (cm^{-1}): 3219 (N–H)), 3140 (Aromatic C–H), 2934 (C^3_{sp}–H), 1651 (C═N), 1601 (C═C), 1280 (C–O); **^{1}H NMR** (700 MHz, DMSO-d_6) δ 13.28 (s, N–H, 1H), 8.45 (s, 1H), 8.24–8.22 (m, 2H), 8.21 (s, 1H), 7.99 (dd, J = 2.0 Hz, 8.4 Hz, 1H), 7.96 (d, J = 2.0 Hz, 1H), 7.89–7.87 (m, 2H), 7.25 (d, J = 8.4 Hz, 1H), 3.95 (s, 3H), 3.90 (s, 3H); **^{13}C NMR** (175 MHz, DMSO-d_6) δ 160.3, 152.5, 149.7, 149.5, 142.2, 142.1, 141.3, 140.8, 140.5, 130.2, 129.9, 129.5, 129.3, 121.8, 121.6, 114.5, 112.4, 111.1, 105.8, 56.2, 56.1; **HRMS** (+ESI) $[M+H]^+$: 357.1362, $C_{21}H_{16}N_4O_2$ requires 357.1351.

2-(2-methoxy-4-nitrophenyl)-1H-imidazo [*4,5-b*]*phenazine* ***(3d)***: Red-brick solid. (87 % yield); M.p. >300 °C; **FTIR** (cm^{-1}): 3426 (N–H), 3089 (Aromatic C–H), 2935 (C^3_{sp}–H), 1618 (C═C), 1522 (–NO_2), 1248 (C–O); **^{1}H NMR** (500 MHz, DMSO-d_6) δ 12.82 (s, N–H, 1H), 8.77 (d, J = 8.5 Hz, 1H), 8.60 (s, 1H), 8.43 (s, 1H), 8.26–8.24 (m, 2H), 8.09 (d, J = 2.0 Hz, 1H), 8.07 (dd, J = 2.0, 8.5 Hz, 1H), 7.91–7.89 (m, 2H), 4.26 (s, 3H); **^{13}C NMR** (125 MHz, DMSO-d_6) δ 164.5, 161.9, 160.5, 142.9, 142.2, 140.8, 140.6, 139.3, 130.4, 130.2, 129.6, 129.5, 129.3, 114.9, 113.6, 108.1, 106.3, 105.3, 102.0, 56.1; **HRMS** (+ESI) $[M+H]^+$: 372.1092, $C_{20}H_{13}N_5O_3$ requires 372.1096.

2-(3-hydroxy-4-nitrophenyl)-1H-imidazo [*4,5-b*]*phenazine* ***(3e)***: Red-brick solid (84 % yield); M.p. >300 °C; **FTIR** (cm^{-1}): 3387 (N–H), 3254 (O–H), 2929 (Aromatic C–H), 1624 (C═C), 1528 (–NO_2), 1314 (C–N); **^{1}H NMR** (500 MHz, DMSO-d_6) δ 13.65 (s, N–H, 1H), 11.49 (s, O–H, 1H), 8.58 (s, 1H), 8.31 (s, 1H), 8.22 (m, 2H), 8.15 (d, J = 8.4 Hz, 1H), 8.16 (d, J = 1.8 Hz, 1H), 7.91–7.89 (m, 2H), 7.90 (dd, J = 1.8, 8.4 Hz, 1H); **^{13}C NMR** (175 MHz, DMSO-d_6) δ 157.9, 152.6, 148.9, 142.6, 142.3, 140.8, 140.3, 140.2, 139.2, 134.9, 130.7, 130.3, 129.6, 129.3, 126.7, 118.7, 118.6, 116.2, 107.1; **HRMS** (+ESI) $[M+H]^+$: 358.0945, $C_{19}H_{11}N_5O_3$ requires 358.0940.

2-(3-bromo-2-hydroxyphenyl)-1H-imidazo [*4,5-b*]*phenazine* ***(3f)***: Yellow-mustard solid (79 % yield); M.p. >300 °C; FTIR (cm^{-1}): 3358 (N–H/O–H), 3037 (Aromatic C–H), 1613 (C═C), 1582 (C═N), 1424 (C–N), 748 (C–Br); **^{1}H NMR** (500 MHz, DMSO-d_6) δ 14.26 (s, N–H, 1H), 13.90 (s, O–H, 1H), 8.61 (s, 1H), 8.36 (s, 1H), 8.27–8.25 (m, 2H), 8.23 (dd, J = 1.4, 7.9 Hz, 1H), 7.94–7.92 (m, 2H), 7.87 (dd, J = 1.4, 7.9 Hz, 1H), 7.10 (t, J = 7.9 Hz, 1H); **^{13}C NMR** (125 MHz, DMSO-d_6) δ 159.6, 156.7, 149.3, 142.8, 142.7, 142.6, 142.5, 142.4, 137.3, 130.7, 130.6, 129.6, 129.5, 127.4, 121.1, 114.9, 113.1, 111.6, 107.2; HRMS (+ESI) $[M+H]^+$: 391.0182, 393.0138 (isotope Br), $C_{19}H_{11}BrN_4O$ requires 391.0194.

2-(3,4,5-trimethoxyphenyl)-1H-imidazo [*4,5-b*]*phenazine* ***(3g)***: Yellow solid (16 % yield); M.p. >300 °C; **FTIR** (cm^{-1}): 3336 (N–H), 3102 (Aromatic C–H), 2941 (C^3_{sp}–H), 1645 (C═N), 1588 (C═C), 1420 (C–N), 1223 (C–O); **^{1}H NMR** (700 MHz, DMSO-d_6) δ 13.35 (s, N–H, 1H), 8.49 (s, 1H), 8.25 (s, 1H), 8.24–8.21 (m, 2H), 7.89–7.88 (m, 2H), 7.72 (s, 2H), 3.97 (s, 6H), 3.80 (s, 3H); **^{13}C NMR** (175 MHz, DMSO-d_6) δ 160.0, 153.8, 149.4, 142.3, 142.1, 141.1, 141.0, 140.7, 140.4, 130.3, 130.1, 129.5, 129.3, 124.3, 114.9, 106.1, 105.7, 60.7, 56.7; **HRMS** (+ESI) $[M+H]^+$: 387.1443, $C_{22}H_{18}N_4O_3$ requires 387.1457.

2-(2,4-dihydroxyphenyl)-1H-imidazo [*4,5-b*]*phenazine* ***(3h)***: Brownish orange solid. (70 % yield); M.p. >300 °C; **FTIR** (cm^{-1}): 3400 (N–H), 3234 (O–H), 3064 (Aromatic C–H), 1653 (C═N), 1631 (C═C), 1433 (C–N); **^{1}H NMR** (700 MHz, DMSO-d_6) δ 13.26 (s, N–H, 1H), 13.00 (s, O–H, 1H), 10.41 (s, O–H, 1H), 8.40 (s, 1H), 8.24–8.23 (m, 2H), 8.21 (s, 1H), 8.04 (d, J = 8.6 Hz, 1H), 7.89–7.87 (m, 2H), 6.55 (dd, J = 2.3, 8.6 Hz, 1H), 6.49 (d, J = 2.3 Hz, 1H); **^{13}C NMR** (175 MHz, DMSO-d_6) δ 163.3, 161.9, 160.7, 147.2, 142.2, 142.1, 140.8, 140.7, 139.4, 130.2, 130.0, 129.9, 129.4, 129.3, 113.3, 109.0, 106.1, 104.1, 103.6; **HRMS** (+ESI) $[M+H]^+$: 329.1035, $C_{19}H_{12}N_4O_2$ requires 329.1039.

2-(4-isopropylphenyl)-1H-imidazo [*4,5-b*]*phenazine* ***(3i)***: Brownish orange solid. (28 % yield); M.p. >300 °C; **FTIR** (cm^{-1}): 3317 (N–H), 3056 (Aromatic C–H), 2959 (C^3_{sp}–H), 2868 (C^2_{sp}–H), 1631 (C═N), 1611 (C═C), 1424 (C–N); **^{1}H NMR** (700 MHz, DMSO-d_6) δ 13.38 (s, N–H, 1H), 8.50 (s, 1H), 8.32 (d, J = 8.4 Hz, 2H), 8.25 (s, 1H), 8.24–8.22 (m, 2H), 7.90–7.89 (m, 2H), 7.56 (d, J = 8.4 Hz, 2H), 1.30 (d, J = 6.9 Hz, 6H), 1.24 (d, J = 6.9 Hz, 1H); **^{13}C NMR** (175 MHz, DMSO-d_6) δ 160.1, 156.1, 153.2, 149.5, 142.2, 141.1, 140.7, 140.4, 134.8, 130.2, 129.9, 129.4, 129.3, 128.4, 127.7, 127.6, 126.9, 115.0, 106.2, 33.9, 24.0; **HRMS** (+ESI) $[M+H]^+$: 339.1610, $C_{22}H_{18}N_4$ requires 339.1610.

2-(4-hydroxyphenyl)-1H-imidazo [*4,5-b*]*phenazine* ***(3j)***: Reddish black solid. (31 % yield); M.p. >300 °C; **FTIR** (cm^{-1}): 3343 (N–H), 3234 (O–H), 3061 (Aromatic C–H), 1611 (C═C), 1502 (C═N), 1427 (C–N); **^{1}H NMR** (500 MHz, DMSO-d_6) δ 13.19 (s, N–H, 1H), 10.35 (s, O–H, 1H), 8.39 (s, 1H), 8.24–8.21 (m, 4H), 8.18 (s, 1H), 7.89–7.87 (m, 2H), 7.03–7.01 (m, 2H); **^{13}C NMR** (175 MHz, DMSO-d_6) δ 161.5, 160.5, 149.9, 142.1, 142.0, 141.4, 140.7, 140.6, 130.3, 130.1, 129.9, 129.4, 129.3, 119.9, 116.5, 114.2, 105.7; HRMS (+ESI) $[M+H]^+$: 313.1086, $C_{19}H_{12}N_4O$ requires 313.1089.

2-(4-(trifluoromethoxy)phenyl)-1H-imidazo [*4,5-b*]*phenazine* ***(3k)***: Yellowish orange solid. (15 % yield); M.p. >300 °C; **FTIR** (cm^{-1}): 3416 (N–H), 3066 (Aromatic C–H), 1653 (C═C), 1617 (C═N), 1215 (C–F); **^{1}H NMR** (700 MHz, DMSO-d_6) δ 13.60 (br s, N–H, 1H), 8.63 (br s, 1H), 8.55–8.53 (m, 2H), 8.34 (br s, 1H), 8.28–8.27 (m, 2H), 7.95–7.93 (m, 2H), 7.73 (d, J = 8.1 Hz, 2H); **^{13}C NMR** (175 MHz, DMSO-d_6) δ 158.7, 151.1, 142.4, 140.7, 130.4, 129.4, 128.4, 122.7, 121.2, 119.8, 118.3, 106.7; **HRMS** (+ESI) $[M+H]^+$: 381.0964, $C_{20}H_{11}F_3N_4O$ requires 381.0963.

2-(2-fluorophenyl)-1H-imidazo [*4,5-b*]*phenazine* ***(3l)***: Yellowish brown solid. (32 % yield); M.p. >300 °C; **FTIR** (cm^{-1}): 3300 (N–H), 3076 (Aromatic C–H), 1619 (C═N), 1532 (C═C), 1425 (C–N), 1219 (C–F); **^{1}H NMR** (500 MHz, DMSO-d_6) δ 13.06 (s, N–H, 1H), 8.58 (s, 1H), 8.44 (td, J = 1.7, 7.7 Hz, 1H), 8.36 (s, 1H), 8.27–8.23 (m, 2H), 7.92–7.89 (m, 2H), 7.76–7.71 (m, 1H), 7.59 (dd, J = 8.4, 10.9 Hz, 1H), 7.51 (td, J = 1.0, 8.0 Hz, 1H); **^{13}C NMR** (125 MHz, DMSO-d_6) δ 161.7, 159.7, 155.4, 148.2, 142.4, 142.2, 140.7, 140.5, 140.1, 134.4, 134.3, 131.5, 130.3, 130.0, 129.5, 129.3, 125.8, 115.5, 107.2; **HRMS** (+ESI) $[M+H]^+$: 315.1049, $C_{19}H_{11}FN_4$ requires 315.1046.

2-(4-fluorophenyl)-1H-imidazo [*4,5-b*]*phenazine* ***(3 m)***: Red brick solid (90 % yield); M.p. >300 °C; **FTIR** (cm^{-1}): 3397 (N–H), 3184 (Aromatic C–H), 1651 (C═C), 1611 (C═N), 1427 (C–N), 1226 (C–F); **^{1}H NMR** (700 MHz, DMSO-d_6) δ 13.47 (s, N–H, 1H), 8.52 (s, 1H), 8.46–8.43 (m, 2H), 8.28 (s, 1H), 8.26–8.23 (m, 2H), 7.91–7.89 (m, 2H), 7.54 (t, J = 8.9 Hz, 2H); **^{13}C NMR** (175 MHz, DMSO-d_6) δ 165.4, 164.0, 159.1, 142.2, 130.8, 130.7, 130.3, 129.3, 125.8, 116.9, 116.8; **HRMS** (+ESI) $[M+H]^+$: 315.1038, 317.1221 (isotope),

$C_{19}H_{11}FN_4$ requires 315.1046.

4.2. Biology

4.2.1. Expression and purification of DENV2 NS2B-NS3 protease

The recombinant DENV-2 NS2B-NS3 protease expression and purification process were carried out according to the methodology described by Heh et al. [49]. The corresponding gene was inserted into the pQE-30 vector (Qiagen, Hilden, Germany) using BamHI and HindIII restriction sites. This pQE-30 construct was then introduced into Escherichia coli XL1-Blue MRF' (Stratagene, La Jolla, California, USA).

To express the DENV-2 NS2B-NS3 protease, a culture of recombinant *E. coli* XL1-Blue MRF' was prepared in Luria-Bertani (LB) medium (pH 7.5), supplemented with 100 μg/mL ampicillin. The culture was incubated at 37 °C in an orbital shaker at 200 rpm for 18 h. A 10 % (v/v) inoculum from this culture was transferred to fresh LB/amp medium and incubated at 37 °C, 200 rpm until the absorbance of the culture medium at 600 nm reached 0.8, as measured using Ultrospec 2100 pro UV/Visible Spectrophotometer (Cytiva, Marlborough, MA, USA). Induction of enzyme expression was achieved by adding 0.5 mM isopropyl-β-D-thiogalactopyranoside (IPTG), followed by further incubation at 37 °C, 200 rpm for 4 h. The culture was then centrifuged at 5000×*g* for 10 min at 4 °C, and the cell pellets were collected. The pellets were resuspended in 30 mL of buffer (20 mM sodium phosphate buffer, 300 mM NaCl, 20 mM imidazole, pH 7.4) and subjected to cell lysis through sonication (4 × 30-s bursts) on ice at 43 % amplitude using Branson Ultrasonics™ Sonifier™ S-450 Digital Ultrasonic Cell Disruptor/Homogenizer (Thermo Fisher Scientific, Rockford, IL, USA). The lysate was subsequently centrifuged (15,000×*g* for 10 min at 4 °C) to collect the cell-free lysate.

The purification of DENV-2 NS2B-NS3 protease was performed using a pre-packed 5.0 mL nickel-nitrilotriacetic (Ni-NTA) HisTrap HP column (Cytiva, Marlborough, MA, USA) equilibrated with 20 mM sodium phosphate buffer, 300 mM NaCl, 20 mM imidazole, pH 7.4. The bound enzyme was eluted using a linear gradient of 20–250 mM imidazole at a flow rate of 1.0 mL/min. Eluted fractions were collected, and their purities were assessed through 12 % (w/v) sodium dodecyl sulphate-polyacrylamide gel electrophoresis (SDS-PAGE) analysis. Fractions containing purified enzyme were pooled and utilized for subsequent analyses.

4.2.2. Protease and substrate optimization assay

The black 96 wells TC multiplate flat bottom plate was purchased from Greiner Bio-One Co, quercetin was purchased from sigma, while Boc-Gly-Arg-Arg-MCA substrate was purchased from Peptide Institute, Inc. The enzyme concentration was determined using NanoDrop spectrometer DeNovix DS-11 series [50].

The assay system included DENV2 NS2B-NS3pro, Boc-Gly-Arg-Arg-MCA as substrate and 200 mM Tris-HCl (pH 8.5) buffer. To determine the highest protease activity at a constant concentration of the substrate (100 μM), a protease optimum assay was conducted. Protease concentrations ranged from 0 to 4.2 μM. Likewise, substrate optimum assay was performed containing constant protease concentration of 3.5 μM, with the substrate concentration varying from 0 to 250 μM. The Tecan M1000 PRO microplate reader was used to observe the amount of 7-amino-4-methylcoumarin (AMC) produced as a relative fluorescence unit (RFU) at 365 nm for excitation and 410 nm for emission.

4.2.3. DENV2 NS2B-NS3 protease inhibition assay

This method followed the protocol established by Rothan et al. [51] with modification. Briefly, a total volume of 100 μL of the reaction contains 3.5 μM purified NS2B-NS3 protease in the standard buffer solution at pH 8.5 (200 mM Tris-HCl) with different concentrations of synthesized imidazole phenazine derivatives in the range of 5.5–700.0 μM were preincubated at 37 °C for 10 min. Subsequently, 150 μM substrate was added and the assay mixtures were incubated at the same temperature for another 1 h. The assay condition was validated by performing both a blank control (100 μL of pH 8.5, 200 mM Tris-HCl buffer only) and a negative control (100 μL 3.5 μM DENV NS2B/NS3 protease and 150 μM substrate Boc-Gly-Arg-Arg-MCA in standard buffer) were carried out simultaneously. The experiments were performed in triplicate (n = 3). As above, the assay was performed using a black 96-well flat-bottom TC multiplate plate format on a Tecan M1000 PRO microplate reader at excitation and emission wavelengths of 365 and 410 nm, respectively. The fluorescence signal was then used to calculate the percentage of inhibition activity of the peptide inhibitors as Equation (1).

$$\%\ of\ enzyme\ activity = \frac{sample - buffer}{negative\ control - buffer} \times 100 \quad (1)$$

$$\%\ of\ inhibition = 100 - \%\ of\ enzyme\ activity$$

4.2.3.1. Statistic. The IC_{50} values were calculated using nonlinear regression models in GraphPad Prism 9.3.1 software.

4.3. Molecular docking study

The binding pose of the 2 most potent imidazole phenazine derivatives, **3e** and **3k**, with the DENV2 NS2B-NS3 protease was carried out by molecular docking. The DENV2 NS2B-NS3pro model was derived from a published article in which the model was constructed utilizing the DENV2 complex cofactor-protease as a base and the crystal structure of the NS2B-NS3pro West Nile virus (WNV) as a template [43]. The 2D structural drawings were created using ChemDraw 19.0 (Cambridge soft Corporation, MA, USA) and

subsequently converted into 3D models using Chem3D 16.0. UCSF Chimera 1.14 is used for interactive visualization and analysis of molecular structures and associated data [52]. The grid box size and grid spacing were set to 22.5 × 22.5 × 22.5 Å around the catalytic triad, with the center set to x = 21.1, y = 44.6, and z = −1.8. The primary docking programmed utilized in this study was AutoDock Vina (The Scripps Research Institute, La Jolla, San Diego, USA) to execute the docking process [53]. The conformations with the lowest free energy of binding and the most populated cluster were selected. Discovery Studio Biovia 2017 (Dassault Systèmes, San Diego, California, USA) was used to verify and modify the receptor and ligand structures after performing the docking procedure. Quercetin was used as a positive control and prepared for simulation in a similar way to **3e** and **3k**.

Author contributions

Unang Supratman: Writing – original draft, Validation, Investigation, Formal analysis. Habibah A. Wahab: Writing – original draft, Validation, Software, Methodology, Funding acquisition. Mohamad Nurul Azmi Mohamad Taib: Writing – review & editing, Visualization, Validation, Supervision, Resources, Project administration, Methodology, Funding acquisition, Conceptualization. Maywan Hariono: Writing – original draft, Software, Methodology, Conceptualization. Iffah Izzati Zakaria: Writing – original draft, Validation, Resources, Methodology, Formal analysis, Conceptualization. Ezatul Ezleen Kamarulzaman: Writing – original draft, Validation, Supervision, Software, Methodology. Andrey A. Mikhaylov: Writing – original draft, Validation, Methodology. Muhammad Hidhir Khawory: Writing – original draft, Resources, Project administration, Funding acquisition, Conceptualization. Nur Sarah Dyana Khalili: Writing – original draft, Methodology, Investigation, Formal analysis, Data curation. Nurul Hanim Salin: Writing – original draft, Supervision, Software, Methodology, Data curation, Conceptualization

Data availability

The data will be made available on request.

Declaration of competing interest

The authors declare that they have no known competing financial interests or personal relationships that could have appeared to influence the work reported in this paper.

Acknowledgement

The authors would like to acknowledge the financial support from the Ministry of Higher Education (MOHE) Malaysia for Fundamental Research Grant (FRGS/1/2020/STG01/MESTECC/4) and MARA Graduate Excellence Programme (GREP). This project was carried out in cooperation between Malaysian Institute of Pharmaceuticals and Nutraceuticals, IPharm, NIBM and NPSO, SCS, Universiti Sains Malaysia.

Appendix A. Supplementary data

Supplementary data to this article can be found online at https://doi.org/10.1016/j.heliyon.2024.e24202.

References

[1] G. Kuno, G.-J.J. Chang, K.R. Tsuchiya, N. Karabatsos, C.B. Cropp, Phylogeny of the genus flavivirus, J. Virol. 72 (1998) 1, https://doi.org/10.1128/JVI.72.1.73-83.1998.
[2] World Health Organization, Dengue situation update 677, Update Dengue Situation Western Pacific Region (3 August 2023). https://cdn.who.int/media/docs/default-source/wpro—documents/emergency/surveillance/dengue/dengue-20230803.pdf?sfvrsn=5160e027_115.
[3] World Health Organization, Disease outbreak news; dengue in the region of the americas. https://www.who.int/emergencies/disease-outbreak-news/item/2023-DON475, 2023.
[4] H. Maus, F. Barthels, S.J. Hammerschmidt, K. Kopp, B. Millies, A. Gellert, A. Ruggieri, T. Schirmeister, SAR of novel benzothiazoles targeting an allosteric pocket of DENV and ZIKV NS2B/NS3 proteases, Bioorg. Med. Chem. 47 (2021), https://doi.org/10.1016/j.bmc.2021.116392.
[5] P. Bharaj, H.S. Chahar, A. Pandey, K. Diddi, L. Dar, R. Guleria, S.K. Kabra, S. Broor, Concurrent infections by all four dengue virus serotypes during an outbreak of dengue in 2006 in Delhi, India, Virol. J. 5 (2008) 1, https://doi.org/10.1186/1743-422X-5-1.
[6] P.F. Wong, L.P. Wong, S. AbuBakar, Diagnosis of severe dengue: challenges, needs and opportunities, Journal of Infection and Public Health 13 (2) (2020) 193–198, https://doi.org/10.1016/j.jiph.2019.07.012.
[7] M.A. Abduraman, M. Hariono, R. Yusof, N.A. Rahman, H.A. Wahab, M.L. Tan, M. Lan, Development of a NS2B/NS3 protease inhibition assay using Alpha Screen Ò beads for screening of anti-dengue activities, Heliyon 4 (2018) 1023, https://doi.org/10.1016/j.heliyon.2018.
[8] S. Chanprapaph, P. Saparpakorn, C. Sangma, P. Niyomrattanakit, S. Hannongbua, C. Angsuthanasombat, G. Katzenmeier, Competitive inhibition of the dengue virus NS3 serine protease by synthetic peptides representing polyprotein cleavage sites, Biochem. Biophys. Res. Commun. 330 (4) (2005) 1237–1246, https://doi.org/10.1016/j.bbrc.2005.03.107.
[9] J. Lescar, D. Luo, T. Xu, A. Sampath, S.P. Lim, B. Canard, S.G. Vasudevan, Towards the design of antiviral inhibitors against flaviviruses: the case for the multifunctional NS3 protein from Dengue virus as a target, Antivir. Res. 80 (2) (2008) 94–101, https://doi.org/10.1016/j.antiviral.2008.07.001.
[10] C. De la Guardia, D.E. Stephens, H.T. Dang, M. Quijada, O.V. Larionov, R. Lleonart, Antiviral activity of novel quinoline derivatives against dengue virus serotype 2, Molecules 23 (3) (2018) 672, https://doi.org/10.3390/molecules23030672.

[11] H. Osman, N.H. Idris, E.E. Kamarulzaman, H.A. Wahab, M.Z. Hassan, 3,5-Bis(arylidene)-4-piperidones as potential dengue protease inhibitors, Acta Pharm. Sin. B 7 (4) (2017) 479–484, https://doi.org/10.1016/j.apsb.2017.04.009.

[12] M. Hariono, S.B. Choi, R.F. Roslim, M.S. Nawi, M.S. Tan, E.E. Kamarulzaman, N. Mohamed, R. Yusof, S. Othman, N.A. Rahman, R. Othman, H.A. Wahab, Thioguanine-based DENV-2 NS2B/NS3 protease inhibitors: virtual screening, synthesis, biological evaluation and molecular modelling, PLoS One 14 (1) (2019), https://doi.org/10.1371/journal.pone.0210869.

[13] T.Y. Fonkui, M.I. Ikhile, P.B. Njobeh, D.T. Ndinteh, Benzimidazole schiff base derivatives: synthesis, characterization and antimicrobial activity, BMC Chemistry 13 (1) (2019), https://doi.org/10.1186/s13065-019-0642-3.

[14] J. Yan, W. Liu, J. Cai, Y. Wang, D. Li, H. Hua, H. Cao, Advances in phenazines over the past decade: review of their pharmacological activities, mechanisms of action, biosynthetic pathways and synthetic strategies, Marine Drugs, MDPI. 19 (2021) 11, https://doi.org/10.3390/md19110610.

[15] R.W. Huigens III, B.R. Brummel, S. Tenneti, A.T. Garrison, T. Xiao, Pyrazine and phenazine heterocycles: platforms for total synthesis and drug discovery, Molecules 27 (2022) 1112, https://doi.org/10.3390/molecules27031112.

[16] H. Hussain, S. Specht, S.R. Sarite, M. Saeftel, A. Hoerauf, B. Schulz, K. Krohn, A new class of phenazines with activity against a chloroquine resistant *plasmodium falciparum* strain and antimicrobial activity, J. Med. Chem. 54 (13) (2011) 4913–4917, https://doi.org/10.1021/jm200302d.

[17] H. Liu, Y. He, H. Jiang, H. Peng, X. Huang, X. Zhang, L.S. Thomashow, Y. Xu, Characterization of a phenazine-producing strain *pseudomonas chlororaphis* GP72 with broad-spectrum antifungal activity from green pepper rhizosphere, Curr. Microbiol. 54 (4) (2007) 302–306, https://doi.org/10.1007/s00284-006-0444-4.

[18] N. Imamura, M. Nishijima, T. Takadera, K. Adachi, M. Sakai, H. Sano, New anticancer antibiotics pelagiomicins, produced by a new marine bacterium *pelagiobacter variabilis. The Journal of Antibiotics* 50 (1) (1997) 8–12, https://doi.org/10.7164/antibiotics.50.8.

[19] A. Eriksson, M. Hermanson, M. Wickström, E. Lindhagen, C. Ekholm, A. Jenmalm Jensen, A. Löthgren, F. Lehmann, R. Larsson, V. Parrow, M. Höglund, The novel tyrosine kinase inhibitor AKN-028 has significant antileukemic activity in cell lines and primary cultures of acute myeloid leukemia, Blood Cancer J. 2 (8) (2012) e81, https://doi.org/10.1038/bcj.2012.28.

[20] J.A. Spicer, S.A. Gamage, G.W. Rewcastle, G.J. Finlay, D.J.A. Bridewell, B.C. Baguley, W.A. Denny, Bis(phenazine-1-carboxamides): structure-activity relationships for a new class of dual topoisomerase I/II directed anticancer drugs, J. Med. Chem. 43 (7) (2000) 1350–1358, https://doi.org/10.1021/jm990423f.

[21] N.H. Salin, M. Hariono, N.S.D. Khalili, I.I. Zakaria, F.G. Saqallah, M.N.A. Mohamad Taib, E.E. Kamarulzaman, H.A. Wahab, M.H. Khawory, Computational study of nitro-benzylidene phenazine as dengue virus-2 NS2B-NS3 protease inhibitor, Front. Mol. Biosci. 9 (2022) 875424, https://doi.org/10.3389/fmolb.2022.875424.

[22] A. Bhatnagar, P.K. Sharma, N. Kumar, A Review on "Imidazoles": their chemistry and pharmacological potentials, International Journal of PharmTech Research 3 (1) (2011) 268–282.

[23] S. De, B. Aamna, R. Sahu, S. Parida, S.K. Behera, A.K. Dan, Seeking heterocyclic scaffolds as antivirals against dengue virus, Eur. J. Med. Chem. 240 (2022) 114576, https://doi.org/10.1016/j.ejmech.2022.114576.

[24] T.H. Sucipto, S. Churrotin, H. Setyawati, F. Martak, K.C. Mulyatno, I.H. Amarullah, T. Kotaki, M. Kameoka, S. Yotopranoto, S. Soegijanto, A new copper (II)-imidazole derivative effectively inhibits replication of denv-2 in vero cell, African Journal of Infectious Diseases 12 (1) (2018) 116–119, https://doi.org/10.2101/Ajid.12v1S.17.

[25] Y. Okano, N. Saito-Tarashima, M. Kurosawa, A. Iwabu, M. Ota, T. Watanabe, F. Kato, T. Hishiki, M. Fujimuro, N. Minakawa, Synthesis and biological evaluation of novel imidazole nucleosides as potential anti-dengue virus agents, Bioorg. Med. Chem. 27 (11) (2019) 2181–2186, https://doi.org/10.1016/j.bmc.2019.04.015.

[26] R. Raut, H. Beesetti, P. Tyagi, I. Khanna, S.K. Jain, V.U. Jeankumar, P. Yogeeswari, D. Sriram, S. Swaminathan, A small molecule inhibitor of dengue virus type 2 protease inhibits the replication of all four dengue virus serotypes in cell culture, Virol. J. 12 (1) (2015) 16, https://doi.org/10.1186/s12985-015-0248-x.

[27] V.K. Vishvakarma, N. Shukla, K. Reetu Kumari, R. Patel, P. Singh, A model to study the inhibition of nsP2B-nsP3 protease of dengue virus with imidazole, oxazole, triazole thiadiazole, and thiazolidine based scaffolds, Heliyon 5 (8) (2019) e02124, https://doi.org/10.1016/j.heliyon.2019.e02124.

[28] C.L. Labrecque, C.N. Hilton, J. Airas, A. Blake, K.J. Rubenstein, C.A. Parish, J.A. Pollock, Identification of phenazine-based MEMO1 small-molecule inhibitors: virtual screening, fluorescence polarization validation, and inhibition of breast cancer migration, ChemMedChem 16 (7) (2021) 1163–1171, https://doi.org/10.1002/cmdc.202000797.

[29] A.M. Mahran, S.S. Ragab, A.I. Hashem, M.M. Ali, A.A. Nada, Synthesis and antiproliferative activity of novel polynuclear heterocyclic compounds derived from 2,3-diaminophenazine, Eur. J. Med. Chem. 90 (2015) 568–576, https://doi.org/10.1016/j.ejmech.2013.12.007.

[30] K. Gobis, H. Foks, K. Bojanowski, E. Augustynowicz-Kopeć, A. Napiórkowska, Synthesis of novel 3-cyclohexylpropanoic acid-derived nitrogen heterocyclic compounds and their evaluation for tuberculostatic activity, Bioorg. Med. Chem. 20 (1) (2012) 137–144, https://doi.org/10.1016/j.bmc.2011.11.020.

[31] G.Y. Gao, W.J. Qu, B.B. Shi, Q. Lin, H. Yao, Y.M. Zhang, J. Chang, Y. Cai, T.B. Wei, A reversible fluorescent chemosensor for iron ions based on 1H-imidazo [4,5-b] phenazine derivative, Sensor. Actuator. B Chem. 213 (2015) 501–507, https://doi.org/10.1016/j.snb.2015.02.077.

[32] A.M. Amer, A.A. El-Bahnasawi, M.R.H. Mahran, M. Lapib, On the synthesis of pyrazino[2,3-b]phenazine and 1H-Imidazo[4,5-b]phenazine derivatives, Monatsh. Chem. 130 (1999) 1217–1225.

[33] Y. Lei, D. Li, J. Ouyang, J. Shi, Synthesis and optical properties of 2-(1H-imidazo [4,5-b] phenazin-2-yl) phenol derivatives, Adv. Mater. Res. 311–313 (2011) 1286–1289. https://doi.org/10.4028/www.scientific.net/AMR.311-313.1286.

[34] S. Lin, L. Yang, A simple and efficient procedure for the synthesis of benzimidazoles using air as the oxidant, Tetrahedron Lett. 46 (25) (2005) 4315–4319, https://doi.org/10.1016/j.tetlet.2005.04.101.

[35] P.T. Anastas, J.C. Warner, Green Chemistry: Theory and Practice, Oxford University Press, By permission of Oxford University Press, New York, 1998, p. 30.

[36] U. Sani, H.U. Na'ibi, S.A. Dailami, *In vitro* antimicrobial and antioxidant studies on *N*-(2- hydroxylbenzylidene) pyridine -2-amine and its M(II) complexes, Nigerian Journal of Basic and Applied Sciences 25 (1) (2018) 81, https://doi.org/10.4314/njbas.v25i1.11.

[37] N.V. Ivanova, S.I. Sviridov, A.E. Stepanov, Parallel solution-phase synthesis of substituted 2-(1,2,4-triazol-3-yl)benzimidazoles, Tetrahedron Lett. 47 (46) (2006) 8025–8027, https://doi.org/10.1016/j.tetlet.2006.09.061.

[38] M. Vojtech, M. Petrušová, E. Sláviková, S. Bekešová, L. Petruš, One-pot synthesis of 2-C-glycosylated benzimidazoles from the corresponding methanal dimethyl acetals, Carbohydr. Res. 342 (1) (2007) 119–123, https://doi.org/10.1016/j.carres.2006.10.019.

[39] A. Rivera, M. Maldonado, J. Ríos-Motta, A Facile and efficient procedure for the synthesis of new benzimidazole-2-thione derivatives, Molecules 17 (7) (2012) 8578–8586, https://doi.org/10.3390/molecules17078578.

[40] A.D. Sonawane, R.A. Sonawane, K.M.N. Win, M. Ninomiya, M. Koketsu, In situ air oxidation and photophysical studies of isoquinoline-fused *N*-heteroacenes, Org. Biomol. Chem. 18 (11) (2020) 2129–2138, https://doi.org/10.1039/d0ob00375a.

[41] A.I. Almansour, R. Suresh Kumar, N. Arumugam, A simple, rapid, expedient and sustainable green strategy for the synthesis of benz-/naphthimidazoles, J. King Saud Univ. Sci. 32 (7) (2020) 3153–3158, https://doi.org/10.1016/j.jksus.2020.09.001.

[42] D.S. Thagriki, Quercetin and its derivatives are potent inhibitors of the dengue virus, Trends in Phytochemical Research 6 (1) (2022) 70–85, https://doi.org/10.30495/tpr.2022.1952053.1244.

[43] K. Wichapong, S. Pianwanit, W. Sippl, S. Kokpol, Homology modeling and molecular dynamics simulations of Dengue virus NS2B/NS3 protease: insight into molecular interaction, J. Mol. Recogn. 23 (3) (2010) 283–300, https://doi.org/10.1002/jmr.977.

[44] Y. Sivasothy, S.Y. Liew, M.A. Othman, S.M. Abdul Wahab, M. Hariono, M.S. Mohd Nawi, H. Abdul Wahab, K. Awang, Natural DENV-2 NS2B/NS3 protease inhibitors from *myristica cinnamomea* king, Trop. Biomed. 38 (2) (2021) 79–84, https://doi.org/10.47665/TB.38.2.044.

[45] S.N. Sulaiman, M. Hariono, H.M. Salleh, S.L. Chong, L.S. Yee, A. Zahari, H.A. Wahab, S. Derbré, K. Awang, Chemical constituents from *Endiandra kingiana* (lauraceae) as potential inhibitors for dengue type 2 NS2B/NS3 serine protease and its molecular docking, Nat. Prod. Commun. 14 (9) (2019), https://doi.org/10.1177/1934578X19861014.

[46] V.K. Vyas, R.D. Ukawala, M. Ghate, C. Chintha, Homology modeling a fast tool for drug discovery: current perspectives, Indian J. Pharmaceut. Sci. 74 (1) (2012) 1–17, https://doi.org/10.4103/0250-474X.102537.

[47] W.W. Phoo, A. El Sahili, Z.Z. Zhang, M.W. Chen, C.W. Liew, J. Lescar, S.G. Vasudevan, D. Luo, Crystal structures of full length DENV4 NS2B-NS3 reveal the dynamic interaction between NS2B and NS3, Antivir. Res. 2020 (2020) 182, https://doi.org/10.1016/j.antiviral.2020.104900.
[48] H. Norshidah, C.H. Leow, K.E. Ezleen, H.A. Wahab, R. Vignesh, A. Rasul, N.S. Lai, Assessing the potential of NS2B/NS3 protease inhibitors biomarker in curbing dengue virus infections: *In silico* vs. *In vitro* approach, Front. Cell. Infect. Microbiol. 13 (2023) 1061937, https://doi.org/10.3389/fcimb.2023.1061937.
[49] C.H. Heh, R. Othman, M.J.C. Buckle, Y. Sharifuddin, R. Yusof, N.A. Rahman, Rational discovery of dengue type 2 non-competitive inhibitors, Chem. Biol. Drug Des. 82 (1) (2013) 1–11, https://doi.org/10.1111/cbdd.12122.
[50] P. Desjardins, J.B. Hansen, M. Allen, Microvolume protein concentration determination using the NanoDrop 2000c Spectrophotometer, JoVE 33 (2010) 1610, https://doi.org/10.3791/1610.
[51] H.A. Rothan, H.C. Han, T.S. Ramasamy, S. Othman, N.A. Rahman, R. Yusof, Inhibition of dengue NS2B-NS3 protease and viral replication in vero cells by recombinant retrocyclin-1, BMC Infect. Dis. 12 (2012) 314, https://doi.org/10.1186/1471-2334-12-314.
[52] E.F. Pettersen, T.D. Goddard, C.C. Huang, G.S. Couch, D.M. Greenblatt, E.C. Meng, T.E. Ferrin, UCSF Chimera-a visualization system for exploratory research and analysis, J. Comput. Chem. 25 (13) (2004) 1605–1612, https://doi.org/10.1002/jcc.20084.
[53] L.R.F. De Sousa, H. Wu, L. Nebo, J.B. Fernandes, M.F.D.G.F. Da Silva, W. Kiefer, M. Kanitz, J. Bodem, W.E. Diederich, T. Schirmeister, P.C. Vieira, Flavonoids as noncompetitive inhibitors of Dengue virus NS2B-NS3 protease: inhibition kinetics and docking studies, Bioorg. Med. Chem. 23 (3) (2015) 466–470, https://doi.org/10.1016/j.bmc.2014.12.015.